Thermomechanical consequences of Cretaceous continent-continent collision in the eastern Alps (Austria): insights from two-dimensional modeling.

Willingshofer, E.; van Wees, J.D.A.M.; Cloetingh, S.A.P.L.; Neubauer, F.

published in
Tectonics
1999

DOI (link to publisher)
10.1029/1999TC900017

document version
Publisher's PDF, also known as Version of record

TECTONICS, VOL. 18, NO. 5, PAGES 809-826, OCTOBER 1999

Thermomechanical consequences of Cretaceous continent-continent collision in the eastern Alps (Austria): Insights from two-dimensional modeling

Ernst Willingshofer, J. D. van Wees, and S. A. P. L. Cloetingh

Faculty of Earth Sciences, Vrije Universiteit, Amsterdam, Netherlands

F. Neubauer

Institut für Geologie und Paläontologie, Universität Salzburg, Salzburg, Austria

Abstract. We use two-dimensional numerical modeling techniques to investigate the thermomechanical consequences of closure of the Meliata-Hallstatt ocean and consequent Cretaceous continent-continent collision in the eastern Alps (Austria). In the modeling a lower plate position of the Austro-Alpine (AA) continental block is adopted during collision with the Upper Juvavic-Silice block. The thermal structure of the lithosphere was calculated for major AA tectonic units (Upper, Middle, and Lower Austro-Alpine) by integration of the transient heat flow equation along an approximately NW-SE cross section east of the Tauern Window. Indications of the rheological evolution of the AA were determined by calculating strength profiles at key stages of the Cretaceous orogeny, making use of the thermal modeling predictions combined with rock mechanics data. Cooling in the upper plate and lower greenschist facies metamorphism within footwall parts of the lower Upper Austro-Alpine (UA) plate, related to SE directed underthrusting of the UA beneath the Upper Juvavic-Silice block at circa 100 Ma, were predicted by the numerical model. The observed pressure-temperature path for deeply buried Middle Austro-Alpine (MA) upper crustal units and their subsequent isothermal exhumation are best reproduced assuming a pressure peak at 95 Ma and exhumation rates ranging between 4 and 7.5 mm yr^{-1}. From the modeling results, we deduce that the temperature evolution during eclogite exhumation is primarily dependent on rates of tectonic movements and largely independent of the mode of exhumation (thrusting versus erosion). Furthermore, very rapid postmetamorphic exhumation of southern Lower Austro-Alpine (LA) units is predicted in order to account for subsequent cooling. This is constrained by $^{40}Ar/^{39}Ar$ data. The cooling paths of MA and LA rocks appear to be primarily controlled by their near-surface positions at the end of the Cretaceous rather than by other processes such as concurrent underthrusting. Upward advection of heat by rapid exhumation induced thermal weakening of the thickened crust. The inferred weakness of the central parts of the orogenic system may play an important role during detachment-related tectonic unroofing, orogenic collapse, and concomitant basin formation (central Alpine Gosau basins).

Paper number 1999TC900017.
0278-7407/99/1999TC900017$12.00

1. Introduction

Major plate reorganizations and the development of a Cretaceous mountain range in present-day central and eastern Europe are related to the opening of the Atlantic Ocean. Complex plate and microplate interactions resulted in continent-continent collisions following the closure of Tethys oceanic realms [e.g., *Frisch*, 1979].

The Austro-Alpine block (AA), a continental element of African affinity, at present covering large areas of the eastern Alps (Austria and eastern Switzerland), represents a series of accreted basement-cover units, stacked during Cretaceous continent-continent collision. According to *Tollmann* [1977], the main AA tectonic units (Upper, Middle, and Lower AA; Figure 1) were aligned from NW (Lower AA) to SE (Upper AA) with the Middle AA in between. They show profound differences in (1) the degree of the Cretaceous thermal overprint and (2) the sedimentary record and stratigraphic range of cover sequences.

Cretaceous metamorphism and deformation within the AA realm (Figure 1) is commonly related to subduction of the South Penninic ocean (Figure 2a) and subsequent collision with the Middle Penninic continental block [*Hawkesworth et al.*, 1975; *Frisch*, 1979; *Tollmann*, 1980; 1987; *Behrmann*, 1990]. This model implies an upper plate position of the AA during the Cretaceous. The widespread Barrovian-type metamorphism within AA basement units was thought to be contemporaneous with high-pressure metamorphism and nappe stacking within Penninic units, together forming a paired metamorphic belt (for review see *Stüwe* [1998] and references therein). Additionally, similar kinematic data (top-to-the-W-NW shearing within the AA as well as Penninic units) were used as an argument for their synchroneity [*Behrmann and Ratschbacher*, 1989; *Behrmann*, 1990]. However, recent structural investigations [*Genser*, 1993; *Kurz et al.*, 1996] clearly showed that top-to-the-west shearing in the footwall Penninic units occurred during peak thermal conditions, circa 27-30 Ma [*Reddy et al.*, 1993; *Inger and Cliff*, 1994], independently from Cretaceous top-to-the-west shearing within the AA units [*Krohe*, 1987; *Frank*,

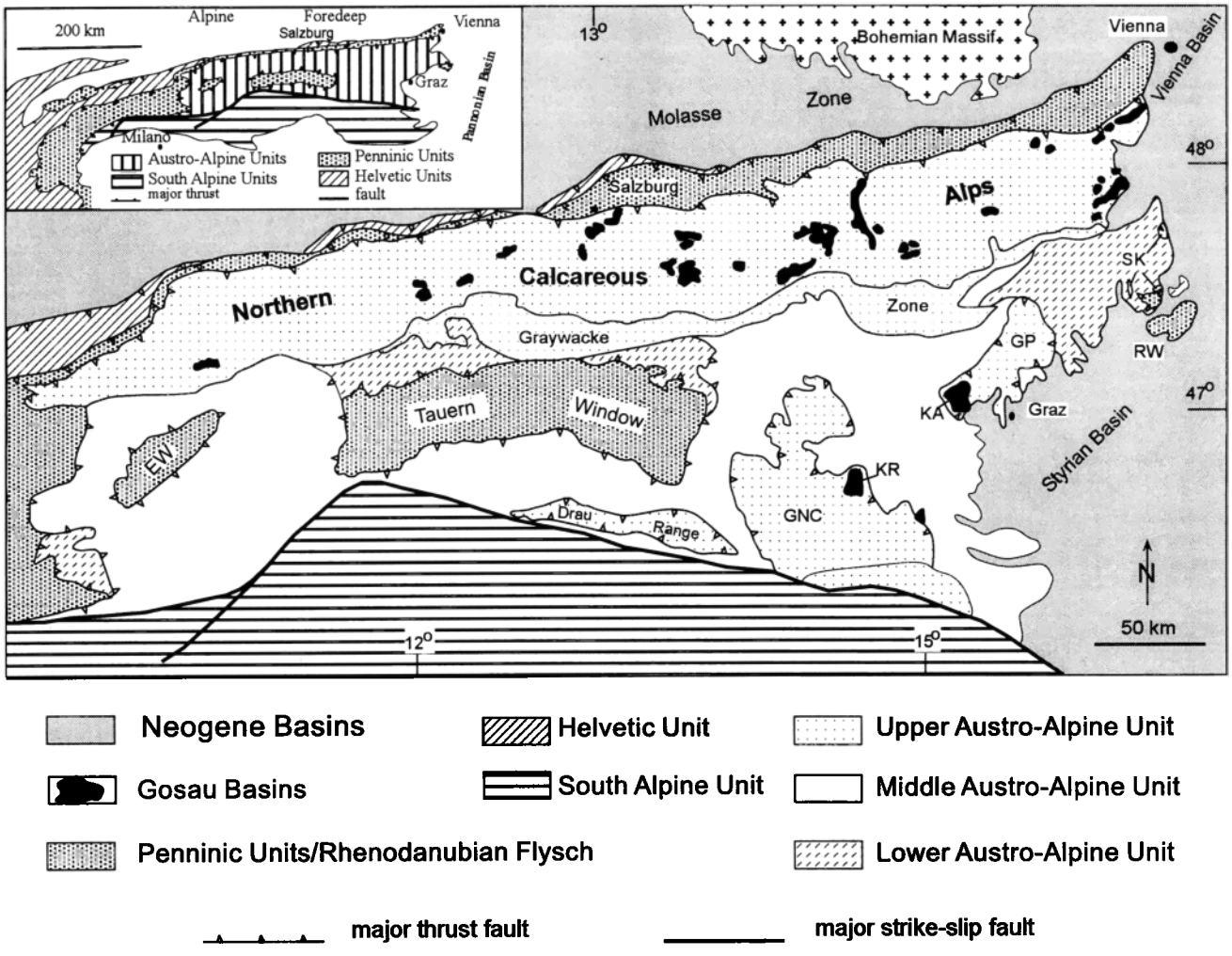

Figure 1. Tectonic map of the eastern Alps showing the main tectonic units of the Alps (inset) and the Austro-Alpine realm. EW, Engadine Window; GP, Graz Paleozoic; GNC, Gurktal nappe complex; KA, Kainach Gosau; KR, Krappfeld Gosau; RW, Rechnitz window group; SK, Sieggraben Klippen.

1987; *Ratschbacher et al.*, 1989; *Neubauer et al.*, 1992a; *Ehlers et al.*; 1994, *Stüwe and Sandiford*, 1995; *Dallmeyer et al.*, 1996].

More recent geochronologic work, carried out on AA eclogites by *Hoinkes et al.* [1991], *Thöni and Jagoutz* [1992], *Thöni and Miller* [1996], and *Dallmeyer et al.* [1996], revealed a Cretaceous age of high-pressure metamorphism, indicating a lower plate rather than an upper plate position of the AA block during Cretaceous orogeny [*Thöni and Jagoutz*, 1992; *Neubauer*, 1994a; *Froitzheim et al.*, 1996; *von Blankenburg and Davies*, 1996]. This fundamental difference led to the development of new models, explaining the thermal evolution of the AA units in terms of Cretaceous continent-continent collision between the Austro-Alpine and the Upper Juvavic-Silice blocks (Figure 2b), after the closure of the Meliata-Hallstatt ocean [*Thöni and Jagoutz*, 1992; *Neubauer*, 1994a; *Froitzheim et al.*, 1996; *von Blankenburg and Davies*, 1996]. The timing of intra-AA crustal thickening by multiple imbrication of basement-cover nappes within different structural levels (Upper, Middle, and Lower Austro-Alpine), as well as synorogenic to late orogenic extension associated with cooling of major basement units, is constrained by an extensive set of $^{40}Ar/^{39}Ar$ data [*Neubauer et al.*, 1995; *Dallmeyer et al.*, 1996, 1998; *Handler et al.*, 1996]. Constraints on the opening, the spreading duration, and the closure of the Meliata-Hallstatt ocean are given by the sedimentary record [e.g., *Kozur*, 1991; *Gawlick*, 1996; *Schweigl and Neubauer*, 1997].

We used the paleogeographic relationships proposed by *Tollmann* [1977], together with pressure-temperature-time (P-T-t) paths and stratigraphic and kinematic data as constraints for our two-dimensional (2-D) numerical model. The thermal and mechanical structure of the lithosphere was calculated along an approximately NW-SE running cross section east of the Tauern Window within a given kinematic frame. Unlike *Genser et al.* [1996], who concentrated on the thermo-mechanical modeling of the Cenozoic evolution of the Penninic units, our major emphasis lies on the thermal and mechanical consequences of Cretaceous continent-continent collision, assuming a lower plate position of the AA in order

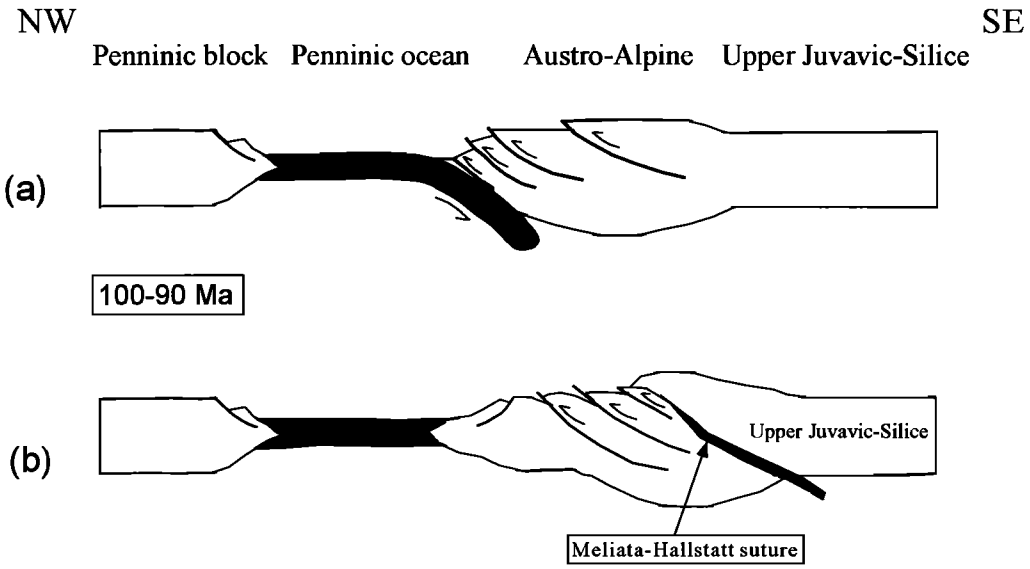

Figure 2. Sketches of different models for the Cretaceous tectonic evolution of the Austro-Alpine (AA) realm: (a) nappe stacking and metamorphism within the AA domain related to subduction of the South Penninic ocean [after *Frisch,* 1979; *Behrmann* 1990] and (b) nappe stacking and metamorphism within the AA domain is related to Cretaceous continent-continent collision between the AA- and the Upper Juvavic-Silice blocks [after *Neubauer*, 1994a].

to explain the observed P-T-t paths within the AA block. Furthermore, the relationship of heat flow and the timing of metamorphic events and the role of lithospheric strength with respect to formation of successor basins are investigated.

2. Tectonostratigraphy and P-T-t Data

In this section we briefly summarize the distinguishing characteristics of AA units. P-T-t data used as constraints for the numerical model are listed in Table 1. P-T-t data on the Cretaceous evolution of the AA realm are also reviewed by *Frank et al.* [1987]; *Genser et al.* [1996], *von Blankenburg and Davies* [1996]; *Stüwe* [1998]; and *Frey et al.* [1999].

2.1. Upper Austro-Alpine (UA)

The UA nappe complex, the uppermost element of the AA nappe edifice, consists of internally imbricated basement-cover nappes (Figure 1). The basement consists of Ordovician to Carboniferous fossiliferous sequences exposed in the Paleozoic of Graz, the Gurktal thrust system and the Graywacke Zone with minor intercalations of crystalline basement in the last. The basement is unconformably covered by Permian to Eocene sequences, most of which are exposed in the Northern Calcareous Alps (NCA) (Figure 1). The sedimentary cover is thought to represent the allochthonous passive margin and basinal sequences of the Meliata-Hallstatt oceanic basin [*Schweigl and Neubauer*, 1997].

In general, Cretaceous P-T conditions within the UA nappe complex did not exceed lower greenschist facies conditions (Figure 3) as indicated by isotopic and illite-crystallinity data [*Kralik et al.*, 1987, and references therein; *Fritz*, 1988]. In the NCA a distinct increase in metamorphic grade from unmetamorphosed in the north to very low to low grade in the south can be recognized [*Kralik et al.*, 1987; *Frey et al.*, 1999] (Figure 3). Intra-UA nappe stacking and related lower greenschist facies metamorphism in the Graywacke Zone was dated by a series of muscovite and whole rock phyllite $^{40}Ar/^{39}Ar$ measurements yielding ages between 98 and 94 Ma [e.g., *Dallmeyer et al.*, 1996; *Handler et al*, 1996].

2.2. Middle Austro-Alpine (MA)

The MA to the footwall of the UA contains imbricated polymetamorphic basement complexes and incomplete Permo-Triassic cover sequences. Most of the MA units were affected by a Cretaceous amphibolite to greenschist facies metamorphism following a high-pressure metamorphic event (Figure 3 and Table 1).

Rocks formed under eclogite facies metamorphic conditions can be traced along a discontinuous and approximately E-W trending zone at the southern margin of the MA throughout the AA block (Figure 3). They are exposed in the Sieggraben unit at the eastern margin of the eastern Alps [*Dallmeyer et al.*, 1992; *Neubauer et al.*, 1999], the Saualpe-Koralpe region [e.g., *Miller*, 1990; *Thöni and Miller*, 1996; *Gregurek et al.*, 1997], the Kreuzeckgruppe near the southeastern corner of the Tauern Window [*Hoke*, 1990], and the Ötztal crystalline, west of the Tauern Window [*Hoinkes et al.*, 1991].

Radiometric data of high-pressure mineral assemblages (Table 1) gave upper and lower age limits of circa 150 and 90 Ma, respectively, for the high-pressure (HP) event with a concentration of ages in the range 100-95 Ma [*Thöni*, 1988;

Table 1. Summary of Austro-Alpine P-T-t Data

	P, GPa	T, °C	Rock Type	Time, Ma	Method	Reference
			Upper Austro-Alpine			
Lower greenschist facies						
Graywacke Zone				98-94	Ar/Ar-Mu	*Dallmeyer et al.* [1996, 1998]
				120-86	K/Ar-Mu	*Kralik et al.* [1987]
NCA southern parts		-320		136-100	K/Ar-Mu	*Kralik et al.* [1987]
			Middle Austro-Alpine			
Eclogite facies						
Sieggraben unit	1.4-1.6	670-750	mafic eclogites			*Dallmeyer et al.* [1992, 1999]
Koralpe-Saualpe	1.8	580-630	mafic eclogites			*Miller* [1990]
			mafic eclogites	95.5 ± 9.5	Sm/Nd-Gt, Om, Phe Phe	*Thöni and Jagoutz* [1992]
			mafic eclogites	95.1 ± 1	Rb/Sr-Phe	*Thöni and Jagoutz* [1992]
	>1.6	700-750	mafic eclogites			*Gregurek et al.* [1997]
	2.0	680	paragneiss	94-88	Sm/Nd-Gt/Wr	*Thöni and Miller* [1996]
	1.4	590	Plattengneiss			*Weber* [1982]
	>1.4	600	Plattengneiss			*Stüwe and Powell* [1995]
	1.1	700	Plattengneiss			*Gregurek et al.* [1997]
Ötztal crystalline/Kreuzeck	1.1-1.2	500-550	basic eclogites			*Hoinkes et al.* [1991]
	>1.0					*Hoke* [1990]
Amphibolite facies						
Sieggraben unit	0.6-0.9	500-600	retrograde eclogite			*Dallmeyer et al.* [1992]
Koralpe-Saualpe	>0.5	600-650	metapelites	90 ± 3	Sm/Nd, Rb/Sr-Gt, Mu, St	*Thöni and Jagoutz* [1992]
	>0.7	575-590	metapelites	90	Sm/Nd-Gt	*Thöni and Miller* [1996]
	0.8-0.9	650-700	amphibolites			*Gregurek et al.* [1997]
Ötztal crystalline	0.5-0.6	600-650	symplectite	90	Rb/Sr-Wr	*Hoinkes et al.* [1991]
			Lower Austro-Alpine			
Amphibolite facies						
Eastern margin of Alps	0.8-0.9	500-550	leucophyllites			*Moine et al.* [1989]
Greenschist facies						
Eastern margin of Alps				82	Ar/Ar-Mu	*Dallmeyer et al.* [1996, 1998]
Vicinity of Tauern Window	0.4-0.45	450	metavolcanics			*Voll* [1977]
	0.8-1.05	350	metasediments	50-37	Ar/Ar-Phe	*Dingeldey et al.* [1997]

For review of cooling paths, see *Frank et al.* [1987] and *Stüwe* [1998]. Mu, muscovite; Gt, garnet; Om, omphacite; Phe, phengite; Wr, whole rock; St, staurolite; Bi, biotite; NCA, Northern Calcareous Alps; P-T-t, pressure-temperature-time.

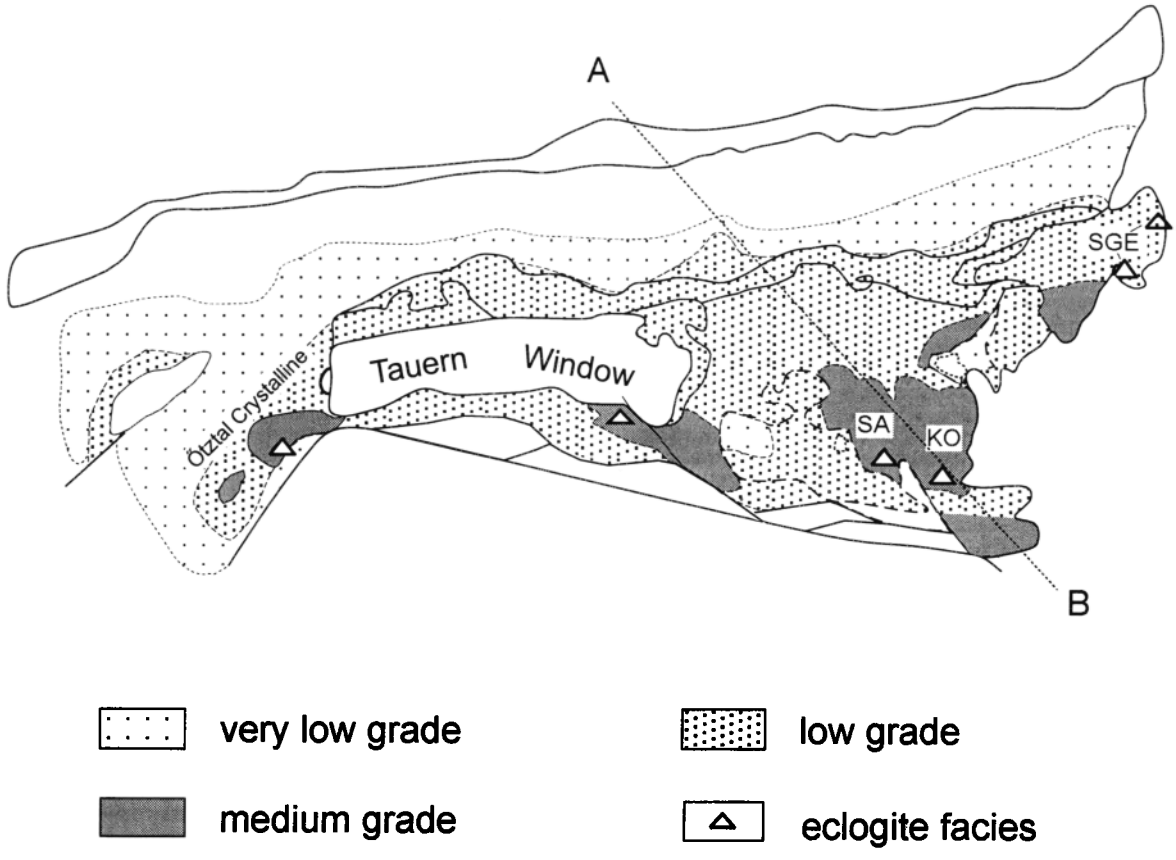

Figure 3. Spatial distribution of Cretaceous metamorphic overprint within the AA, redrawn from *Genser et al.* [1996] and modified after *Frey et al.* [1999]. SA, Saualpe; KO, Koralpe; SGE, Sieggraben eclogites. A-B marks the position of the modeled cross section.

Hoinkes et al., 1991; *Thöni and Jagoutz*, 1992, 1993; *Thöni and Miller*, 1996].

Similar to the UA unit, an increase in metamorphic grade from greenschist in the north-northwest to amphibolite facies in the south-southeast can be recognized. The widespread amphibolite facies metamorphism clearly overprinted the HP event and took place at approximately 90 Ma [*Frank et al.*, 1983, 1987; *Hoinkes et al.*, 1991; *Dallmeyer et al.*, 1992; *Thöni and Jagoutz*, 1992; *Thöni and Miller*, 1996; *Gregurek et al.*, 1997].

A vast number of cooling-related petrological [e.g., *Ehlers et al.*, 1994] and geochronological data from the entire MA complex show that large parts of the MA had already cooled below approximately 100°C by the end of the Cretaceous to Paleogene (50 Ma) [*Frank et al.*, 1976, 1983, 1987; *Morauf*, 1982; *Thöni and Hoinkes*, 1987; *Dunkl*, 1992; *Neubauer et al.*, 1995; *Dallmeyer et al.*, 1996; *Hejl*, 1997].

2.3. Lower Austro-Alpine (LA)

The lowermost AA subunit is the LA unit, which consists of polymetamorphic basement and Permian-Triassic cover sequences in the east and Permian-Lower Cretaceous cover sequences in the west representing the northwestern passive margin of the AA microcontinent, facing the South Penninic ocean.

Table 2. Material Parameters and Rheological Stratification of the Model Section

Layer	Thickness, km	Density ρ, kg m^{-3}	Conductivity κ, W m^{-1}°C^{-1}	Specific Heat c_p, J kg^{-1}°C^{-1}	Heat Production A, mW m^{-3}	Rheology
Upper crust	16	2800	2.6	1050	2.0	wet quartz
Lower crust	16	2800	2.6	1050	0.5	wet diorite
Mantle		3300	3.1	1050	0	olivine

Thermal parameters are after *Pollak and Chapman* [1977]; rock analogues are after *Carter and Tsenn* [1987].

At the eastern margin of the eastern Alps, lower amphibolite facies metamorphic conditions in southern parts of the LA (Figure 3) [*Moine et al.*, 1989; *Neubauer et al.*, 1992a; *Frey et al.*, 1999] were reached before 77 Ma [*Dallmeyer et al.*, 1996; 1998], probably contemporaneous with the greenschist facies metamorphism farther to the north [e.g., *Wieseneder*, 1972] circa 82 Ma [*Dallmeyer et al.*, 1996]. Zircon as well as apatite fission track data in the range 70-60 Myr indicate rapid cooling of the rocks during the Upper Cretaceous [*Dunkl*, 1992].

Recently, greenschist and even blueschist facies metamorphic conditions have been assessed for LA cover series at the Radstadt Tauern area [*Voll*, 1977] and the Tarntal Mountains at the northwestern corner of the Tauern Window [*Dingeldey et al.*, 1997], respectively. The $^{40}Ar/^{39}Ar$ dating gave exclusively Eocene ages for the blueschist event implying that final closure of the South Penninic ocean could not have occurred prior to this event.

3. Numerical Model

We used a two-dimensional finite difference model similar to that of *van Wees et al.* [1992] and *Genser et al.* [1996] to calculate the thermal and mechanical structure of the lithosphere through time by integration of the heat conduction equation

$$\frac{\delta T}{\delta t} = \frac{1}{\rho c_p}\left[\nabla(k\nabla T) + A\right] - v\nabla T \qquad (1)$$

where T is temperature, t is time, ρ is density, cp is specific heat, k is thermal conductivity, A is radiogenic heat production and v is the velocity of tectonic movements. Here the numerical model is used as a tool to evaluate the conditions in terms of heat flow, timing of events, and rates of tectonic movements, required to reproduce observed P-T-t paths within an assumed kinematic frame.

The rectangular-shaped model covers an area of 1800 km in length by 250 km in depth with a grid spacing of 4.5 by 2.5 km, respectively. A model of continental lithosphere is adopted consisting of a 16 km thick upper crust, an equally thick lower crust, and a subcrustal lithosphere. The lithosphere-asthenosphere boundary is defined by a temperature of 1325°C, corresponding to the melting temperature of ultramafic rocks, and is allowed to migrate according to the imposed tectonic movements and resulting temperature change. Furthermore, a constant heat flux across the lithosphere-asthenosphere is assumed. Following *Pollack and Chapman* [1977], we assume that radiogenic heat production within the upper crust accounts for 40% of the surface heat flow. The initial steady state geotherm is determined on the basis of the heat flow assumptions mentioned above. The left- and right-hand sides of the numerical model are fixed ($\delta T/\delta x$ = 0) during time integration. The surface temperature is taken to be zero. Material parameters used for the thermal modeling are listed in Table 2.

The model is capable of simulating simple shear, pure shear, as well as combined shear tectonics, based on a velocity field approach [*Buck et al., 1988*; *van Wees et al.*, 1992, Figure 5]. Blocks separated by a fault move parallel to the fault plane with different constant horizontal velocities during time integration. The vertical velocity component depends on the dip of the fault plane. Bending of the layers where dips change is accommodated by vertical shear [*van Wees et al.*, 1992].

The numerically modeled temperature and material structures are used to calculate two-dimensional strength profiles through the lithosphere based on extrapolation of rock mechanics data [*Carter and Tsenn*, 1987]. A constant strain rate of 10^{-14} s^{-1} and compressional deformation were assumed.

4. Basic Assumptions

In this section, kinematic and heat flow assumptions adopted for the numerical modeling that rely upon geological data and their interpretation are outlined. They are summarized in Table 3. An attempt was made to match kinematics used for the numerical model study closely to those deduced from geological information (see Table 3). Although this paper focuses on the Cretaceous tectonothermal evolution of the AA microcontinent, it is also necessary to account for pre-Cretaceous tectonic events since the Early Cretaceous thermal structure is a function of the preceding tectonics. The numerically modeled cross section to the east of the Tauern Window runs NW-SE, subparallel to the Cretaceous transport direction (Figure 3).

The numerical model starts in the latest Permian (260 Ma). Opening of oceanic basins (Meliata and South Penninic) is modeled by pure shear extension. Sedimentation of the cover series throughout the Mesozoic is simulated by gradually adding sediments on top of the lithosphere to a maximum thickness of 4.5 km. Simple shear kinematics were used for subduction of the oceanic parts (e.g., Figure 4a) as well as the internal imbrication of the AA microcontinent. A progressively increasing angle of subduction, to a maximum dip of 40°, was used to mimic the geometry of a downbending plate. Intra-AA stacking was simulated by footwall propagation of the subduction zone (Figures 5a and 5b) [see also *Davy and Gillet*, 1986] assuming inherited weakness zones crosscutting the AA crust subparallel to the Meliata subduction zone. Underthrusting of the MA that reached its maximum burial depth at 95 Ma followed burial of the UA. Subsequent exhumation of UA and MA rocks was modeled by reversing the sense of movement on the subduction/thrust faults (Figures 5b and 5c) and during a later stage by erosion (Table 3 and Figure 5d). For both mechanisms a velocity has to be defined in the numerical model which may vary laterally in the case of erosion. The change of the exhumation mechanism was adopted in order to maintain correct tectonostratigraphic relationships between tectonic units. However, it is important to note that the choice of the exhumation mechanisms adopted for the numerical modeling does not contradict field observations (see Table 3) and has a minor effect on the model predictions as outlined in section 5.2. Rapid exhumation of eclogites terminated in an amphibolite facies metamorphism. Tectonic unroofing of the MA basement is accounted for by removing the UA unit toward the northwest accompanied by erosion. This phase is intrinsically linked to the preceding one. Further shortening

Table 3. Summary of Tectonothermal Events in the Austro-Alpine and Representative Kinematics Used in the Numerical Model

Time, Ma	Numerical Model Kinematics	Tectonothermal Events Based on Geological Evidence	References
260	start	onset of extension; initial subsidence, volcanism and evaporites	*Lein*[1987], *Kozur* [1991]
230	350 km pure shear extension	rifting and opening of Meliata-Hallstatt ocean (SE of AA); on passive margin; built-up of carbonate platform; in basin; pelagic limestones, ophiolites	*Lein* [1987], *Kozur* [1991], *Channel and Kozur* [1997]
200	thermal relaxation	no rifting; passive margin; dominant carbonate sedimentation; basin: cherty limestones, shales	*Lein* [1987], *Schweigl and Neubauer* [1997], *Kozur* [1991], *Channell and Kozur* [1997]
160	250 km pure shear extension	opening of South Penninic ocean (NW-N of AA); breccias, mafic intrusions	*Kurz et* al. [1998]
	250 km simple shear compression	onset of subduction Meliata-Hallstatt ocean; flysch sedimentation	*Kozur* [1991]
120	390 km simple shear compression	subduction of Meliata-Hallstatt ocean, first collisional events; development of peripheral foreland basin (Rossfeld Basin)	*Kozur* [1991] *Schweigl and Neubauer* [1997]
100	105 km simple shear compression	thrusting and folding in NCA	*Schweigl and Neubauer* [1997]
95	116 km simple shear compression (MA)	subduction of MA; HP metamorphism	for example *Thöni and Miller* [1996]
	exhumation UA by thrusting (8-1.3 km) *	thrusting and lower greenschist facies metamorphism in Graywacke Zone (UA)	*Dallmeyer et al.* [1996]
91	exhumation MA by thrusting (47-28.8 km)*	emplacement of eclogite-bearing unit on lower grade crystalline unit	*Krohe* [1987]
	exhumation UA by thrusting (8-1.3 km)*	thrusting in Graywacke Zone	*Dallmeyer et al.* [1996]
90	exhumation MA by erosion (13 km)+	end of isothermal exhumation phase, amphibolite facies metamorphism	*Thöni and Jagoutz* [1992], *Thöni and Miller* [1996]
	exhumation UA by erosion (5.7 km)+	erosion of NCA; deposition of detritus in; for example Branderfleck Formation	*Oberhauser* [1995], *von Eynatten et al.* [1996]
87	exhumation MA by erosion (10 km)+ thrusting UA (103 km)+	tectonic unroofing of AA and related amphibolite facies metamorphism as above	*Frank* [1987]
82	138 km simple shear compression exhumation MA by erosion (4.3 km)+	thrusting and metamorphism of LA and cooling of MA basement	for example, *Dallmeyer et al.* [1998]
80	exhumation MA by erosion (7.2 km)+ exhumation LA by erosion (20 km)+	cooling and exhumation of MA basement	*Morauf* [1982], *Frank et al.* [1987], *Neubauer et al.* [1995]
	40 km simple shear compression	onset of subduction of South Penninic ocean	*Dallmeyer et al.* [1998]
77	exhumation MA by erosion (1 km)+	cooling and exhumation of MA basement	*Morauf* [1982], *Frank et al.* [1987], *Dunkl* [1992]
	exhumation LA by erosion (8 km)+	cooling and thrusting LA	*Neubauer et al.* [1995], *Dallmeyer et al.* [1998]
	60 km simple shear compression	subduction of South Penninic ocean	
65	exhumation MA by erosion (0.5 km)+	cooling and exhumation of MA basement	*Morauf* [1982], *Frank et al.* [1987], *Dunkl* [1992]
	exhumation LA by erosion (1.5 km)+	cooling and thrusting LA	*Neubauer et al.* [1995], *Dallmeyer et al.* [1996]
	220 km simple shear compression	subduction of South Penninic ocean	*Hejl* [1997], *Dallmeyer et al.* [1998]

AA, Austro-Alpine; HP, high-pressure.

* In case of exhumation by thrusting, the value in parentheses is the amount of motion parallel to the fault plane and the corresponding amount of net vertical motion.

+ The value in parentheses is the amount of net vertical motion due to erosional denudation.

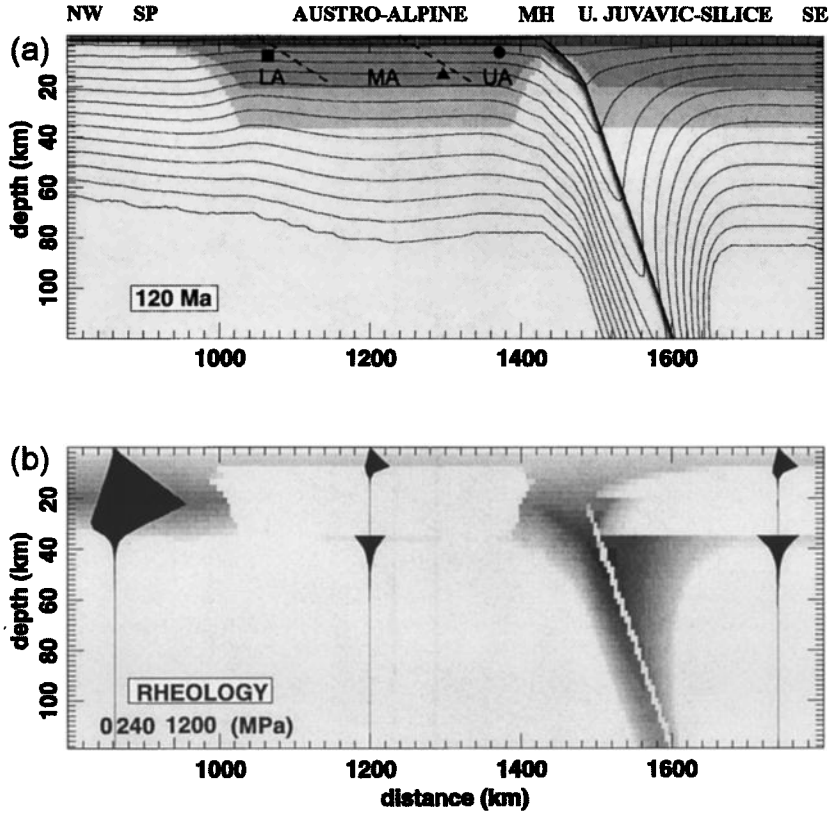

Figure 4. Model configuration 120 Myr ago. (a) Configuration after the closure of the Meliata-Hallstatt ocean (MH) and the Mid-Jurassic opening of the South Penninic ocean (SP) along the NW-SE running model cross section. Shading (from hangingwall to footwall) depicts sedimentary layer, upper crust, lower crust, and subcrustal lithosphere, respectively. Isotherms have a spacing of 100°C. Dashed lines mark the positions of future thrust planes, separating the major Austro-Alpine tectonic units. Symbols represent rocks for which the pressure-temperature (P-T) history was traced through time: circle, Graywacke Zone (Upper Austro-Alpine); triangle, eclogite of the Saualpe-Koralpe region (Middle Austro-Alpine); square, southern part of Lower Austro-Alpine crystalline. (b) Rheological stratification of the lithosphere for the configuration described in Figure 4a and according to the rheological layering listed in Table 2, using a strain rate of 10^{-14} s^{-1} and compressional deformation. Superimposed strength envelopes are displayed for a better visualization of the integrated strength profiles. Dark and light shading depicts strong and weak areas, respectively. Linear grey scale with a maximum of 2 GPa. Same grey scale for all strength envelopes. Note the distinct lateral changes of lithospheric strength.

was accommodated by underthrusting of the LA unit (Figure 5f) and, in a later stage, by the onset of subduction of the South Penninic ocean (Figure 5g). Erosion was used as the exhumation mechanism for LA and MA rocks until the end of the Cretaceous (e.g., Figure 5h). Because there are no lower crustal rocks exposed within the AA block, to the east of the Tauern Window, we assume in our model that the lower crust stays attached to the subducting mantle lithosphere [see also *Wijbrans et al.*, 1993].

An initial surface heat flow of 78 mW m^{-2} was adopted for the thermal calculations. This particular value was chosen to account for the contemporaneity of metamorphism and deformation in the AA. In section 5, model results are summarized for the AA subunits separately to emphasize the major tectonothermal differences of the particular units, according to the kinematics outlined above. Furthermore, changes in heat flow assumptions and the timing of the HP event are explored. Numerically modeled P-T-t paths of grid nodes that are thought to be representative for rocks of particular AA subunits are shown graphically (Figures 6a-6d).

5. Model Results

5.1. Upper Austro-Alpine

Cretaceous continent-continent collision following the closure of the Meliata-Hallstatt ocean starts in our numerical model at 120 Ma (Figure 4a). The thermal regime at that time is completely controlled by the subduction process at the southern margin of the AA; however, we still recognize a gentle upwelling of the isotherms in the area of the South Penninic ocean as a consequence of its Mid-Jurassic opening (Figure 4a). With the onset of collision the UA unit follows

the subducting slab and underthrusts the Upper Juvavic-Silice plate until it reaches its maximum burial depth 100 Myr ago (Figures 5a and 6a). The model geometry for the above mentioned underthrust event was chosen in such a way that the predicted P-T conditions gradually increase toward the SE in agreement with field data (Figure 5a).

Subsequent exhumation of the UA domain by thrusting is accompanied by advective heat transport upward counteracting cooling during contemporaneous subduction of the MA (Figure 5b). Therefore a separate temperature peak is predicted by the numerical model (Figure 6a). The shape of the modeled P-T path during decompression is very much dependent on the velocities used (Figures 5c, 5d, and 6a). Slow exhumation (0.55 mm yr^{-1}) from the thermal peak until 91 Ma is marked by slow cooling (Figure 6a), whereas rapid exhumation until 90 Ma is nearly isothermal (Figure 6a). However, during this phase (100-90 Myr) of UA evolution, predicted temperatures are sufficiently high to open the $^{40}Ar/^{39}Ar$ system for white mica (Figure 6a) and to cause lower greenschist facies metamorphism. Tectonic unroofing of the MA basement by surface-parallel motion of the UA nappe complex toward the NW (Figure 5e) caused a dramatic temperature decrease within UA units (see Figure 5e and 6a). Initial exhumation in the area of the coevally rising MA is followed by an apparent thickening event, which is a function of the model geometry (Figure 6a). Kinks in the modeled P-T path can be related to changing dips of the detachment (compare Figures 5e and 6a). Complete reequilibration of the isotherms at the leading edge of the UA is prohibited by subsequent underthrusting of the LA continental crust and the South Penninic ocean (Figures 5f and 5g). The latter resulted in a short-lived cooling phase (Figures 5g and 6a). In general, burial of UA units after its emplacement towards the NW (Figure 5e) is related to the deposition of overstep sequences (Gosau sediments) on top of the lithosphere (Figure 6a).

5.2. Middle Austro-Alpine

We have investigated the effect of various heat flow assumptions on P-T paths and their relationship to the timing of the eclogite facies metamorphism. For all model runs, rates of tectonic movements are the same. A direct correlation of deformation and the HP metamorphic event is predicted with initial surface and basal heat flow values of 78 and 38.8 mW m^{-2}, respectively (Figure 6b). The use of lower initial surface and basal heat flow values (70, 34 and 60, 28 mW m^{-2}) argue for the necessity of thermal relaxation phases in the order of 5 and 15 Myr, respectively, until observed P-T conditions are reached (Figure 6b). Thus the time when rocks reach their maximum burial depth does not correspond to the time of maximum P-T conditions, implying an earlier onset of the burial history and the temporal separation of deformation and metamorphic events.

Insights on the timing of the HP event as well as on the rates of exhumation required to match the proposed isothermal exhumation path are gained by varying the exhumation duration (Figure 6c). For all model calculations an initial surface heat flow of 78 mW m^{-2} was adopted and we prescribed the regional amphibolite facies metamorphism at the end of the exhumation phase to have occurred at 90 Ma. For simplicity we have adopted thrusting as the only mechanism for eclogite exhumation. In our best fit model (BFM) we reach the pressure peak at 95 Ma (Figure 6c). The thermal consequences of an earlier pressure peak on the subsequent exhumation history are shown in Figure 6c. In order to preserve HP mineral assemblages, only a slight increase in temperature is allowed during their exhumation. Hence the probability of loosing the HP memory distinctly increases by prolonging the exhumation duration (Figure 6c). According to our model results, a time span of 5-10 Myr for eclogite exhumation (exhumation rates of 7.5-4 mm yr^{-1}) gives a good fit with the P-T-t data. Fixing the P peak at 105 Ma or 125 Ma corresponding to exhumation periods of 15 and 35 Myr and exhumation rates of 2.4 and 1 mm yr^{-1}, respectively, results in too high temperatures and in a nearly granulite facies metamorphic overprint after the major decompression phase (Figure 6c).

According to the kinematics outlined in section 4, we adopted a two-step exhumation history for the eclogites. The combination of thrusting (95-91 Myr, Figure 5c) and erosion (91-90 Myr, Figure 5d) led to an isothermal exhumation of the HP rocks. Exhumation rates of 7.2 and 7.8 mm yr^{-1} were deduced for these steps, respectively. It is important to note that although we used different exhumation mechanisms, no significant differences in the predicted P-T paths can be observed (Figure 6b). In the absence of shear heating the shape of the P-T path appears to depend primarily on the velocities of tectonic processes (see also Figure 6c) and not on the exhumation mechanisms used. As mentioned in section 4, we adopted erosional unroofing for the above mentioned second step, although tectonic unroofing may have played an important role. The thermal structure of the lithosphere clearly reflects the decompression history such that a pronounced upwelling of the isotherms can be observed in the area of maximum vertical movements (Figure 5d).

Continuous exhumation of the MA is related to the unroofing of the AA (Figure 5e). In fact, this tectonically induced denudation is thought to be directly related to the amphibolite facies metamorphism occurring around 90 Ma. Underthrusting of buoyant LA crust causes cooling at the base of the hot MA and UA domain but does not influence the temperature evolution of the exhuming eclogites (Figure 5f). The cooling effect of the underthrusting nappe is restricted to a relatively narrow zone in the vicinity of the thrust fault. Although slow exhumation of the eclogites (0.8 mm y^{-1}) is assumed during this time interval, they show rapid cooling triggered by their "near-surface" position (Figures 5f and 6b). Further cooling of the MA basement is influenced by rapid exhumation of LA rocks, which advects heat, slowing down the cooling process of the hangingwall MA rocks. In order to compensate this effect, higher exhumation rates (3.5 mm y^{-1}) were adopted to explain cooling of the rocks through the cooling range of biotite for the Rb-Sr system at 80 Ma (Figure 6b). Final cooling until the end of the Cretaceous is accompanied by slow exhumation of the MA unit (Figures 5h, 5i, and 6b).

5.3. Lower Austro-Alpine

We have treated the LA unit as a single crustal segment, hence maximum P-T conditions are reached in the northern and southern parts at the same time (82 Ma, Figure 5f). Peak

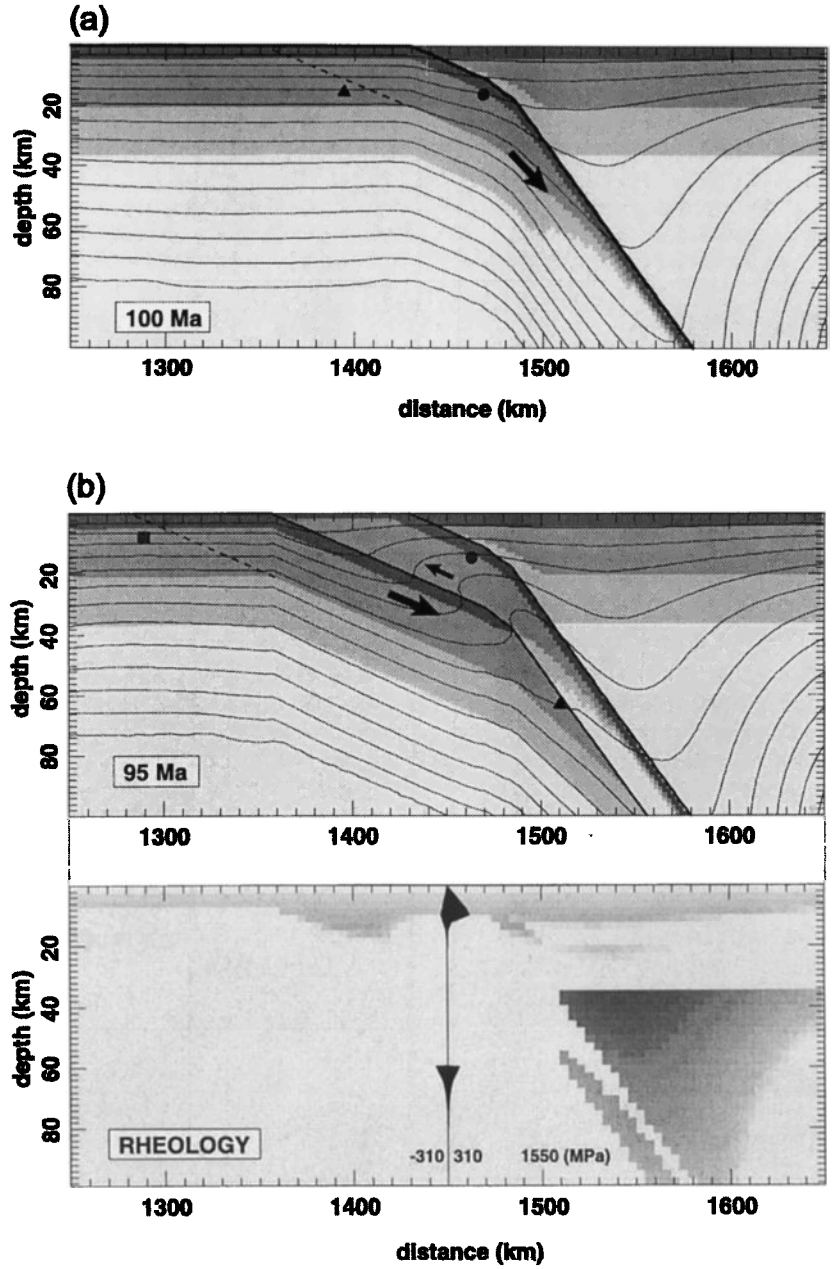

Figure 5. Albian to Maastrichtian model configurations: (a) upper Albian (100 Ma) model geometry after continent-continent collision started and the Upper Austro-alpine (UA) unit was underthrusted underneath the Juvavic-Silice plate; (b) upper Cenomanian (95 Ma), when the UA was underthrusted by the Middle Austro-Alpine (MA); (c) middle Turonian (91 Ma), after the first step of eclogite exhumation by thrusting; (d) upper Turonian (90 Ma), after the second step of exhumation by erosion; (e) Coniacian (87 Ma), after extensional unroofing of the AA basement and orthwestward displacement of the UA; (f) lower Campanian (82 Ma), after underthrusting of the LA unit; (g) late Lower Campanian (80 Ma), after underplating of the South Penninic ocean started and rapid exhumation of the LA basement by erosional denudation; (h) middle Campanian (77 Ma), showing further exhumation of the AA by erosion contemporaneous with underplating of the South Penninic ocean; and (i) Cretaceous-Tertiary boundary (65 Ma), with still ongoing underplating of the South Penninic ocean and slow erosional denudation of the AA basement. Dashed lines mark boundaries between major AA units. Arrows indicate directions of relative motions. The size of the arrows relates to the relative amount of motion with respect to each other. Shading of rheological stratifications of Figures 5b, 5d, and 5f is the same as that in Figure 4b.

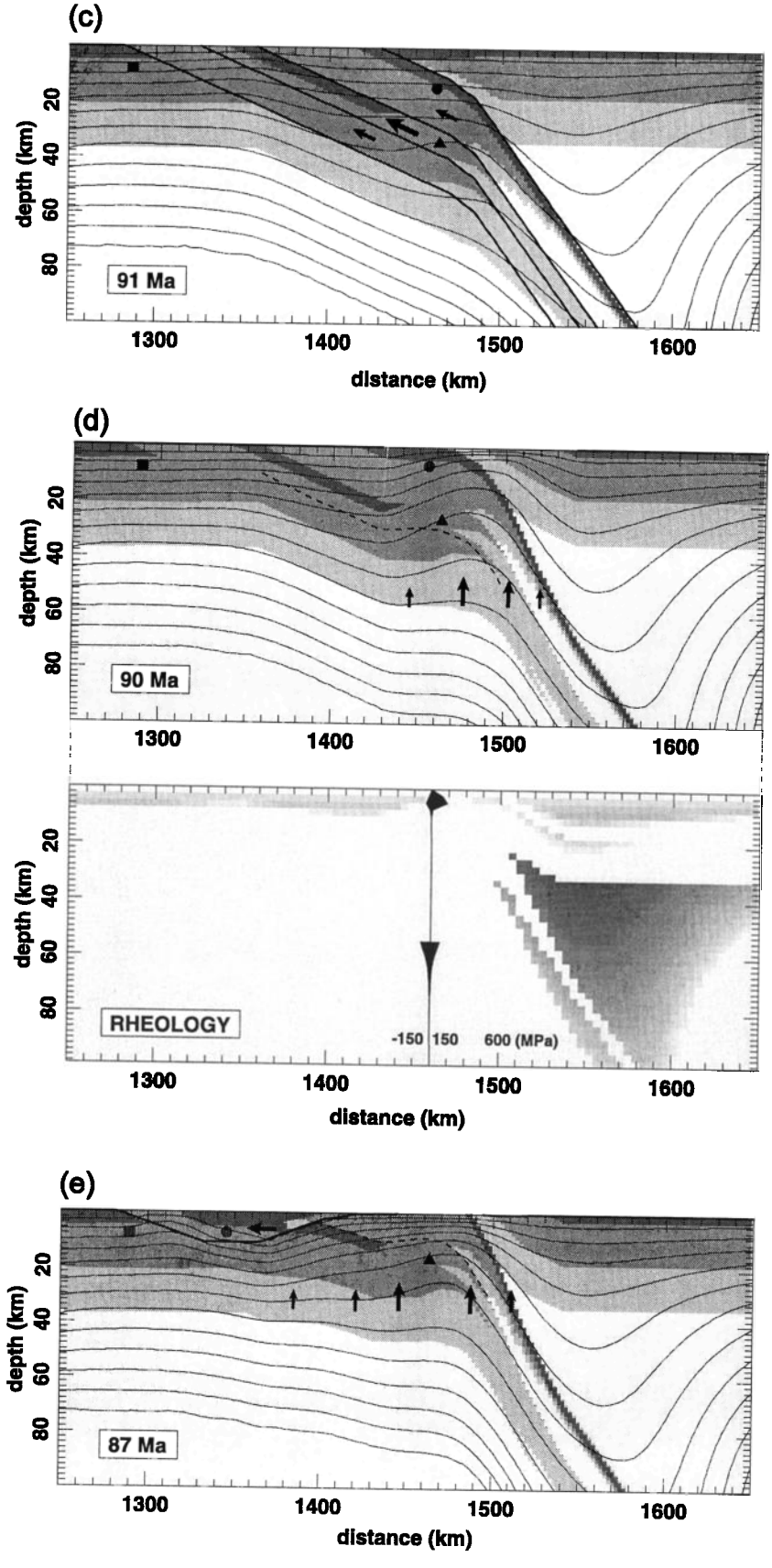

Figure 5. (continued)

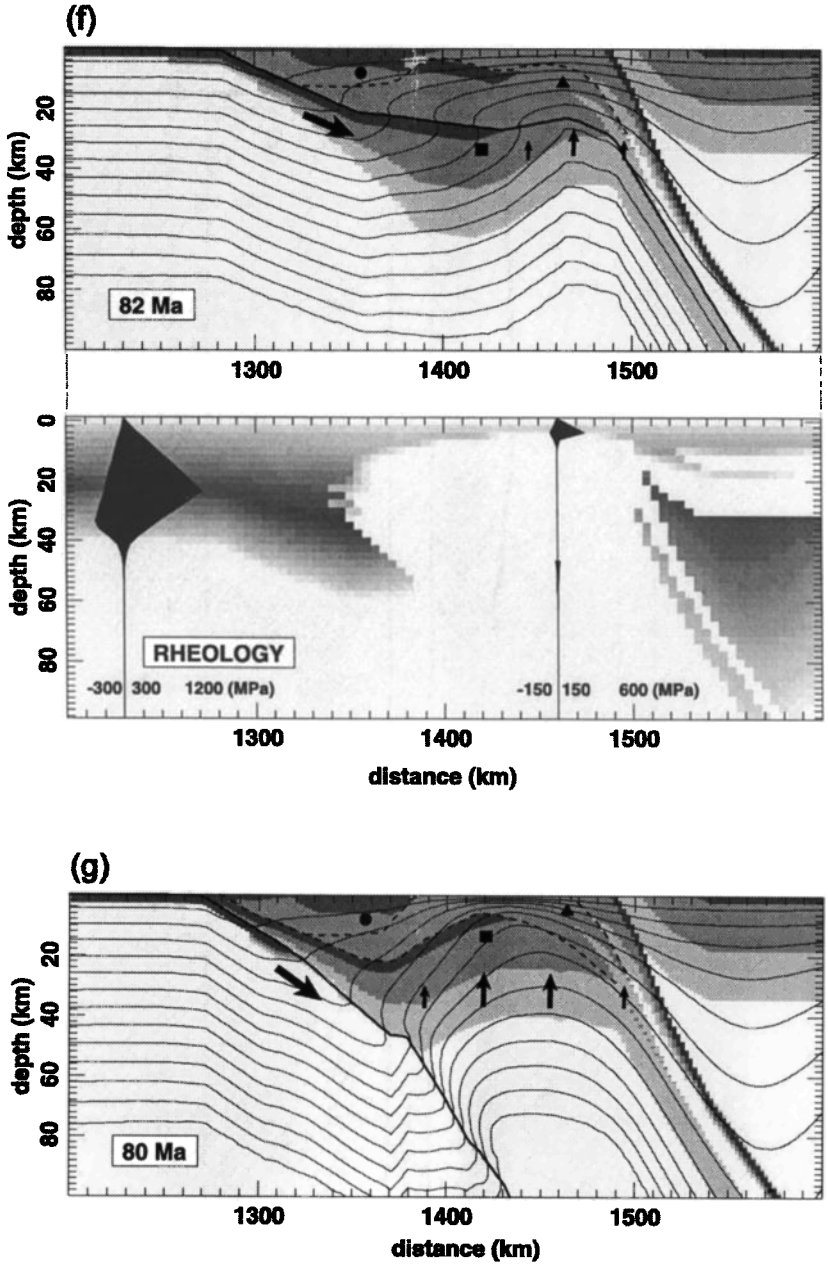

Figure 5. (continued)

metamorphic conditions for southern parts, discussed in section 2.3, essentially correspond to our pressure maximum (Figure 6d). Even very fast exhumation (10 mm y^{-1}) of these rocks is accompanied by a temperature increase and results in a separate temperature peak at considerably lower pressures (Figures 5g and 6d). Subduction of the South Penninic ocean started in our numerical model after deformation was locked in the AA system (80 Ma), thus postdating accretion of the LA complex (Figure 5g). Associated cooling of footwall portions of the LA unit by the subduction process has no influence on the exhumation path of the particular rock particle traced in this model (Figure 6d).

Prescribed ongoing erosional denudation caused further exhumation of LA basement rocks. At this time only moderate exhumation (2.6 mm yr^{-1}) of LA basement is required in order to induce cooling through the temperature range of the $^{40}Ar/^{39}Ar$ system for phengitic white mica at 77 Ma (Figure 6d). Subsequent reequilibration of the isotherms during the last stage of the numerical model run is expressed by moderate cooling of the basement units (Figures 5i and 6d).

In our model, final consumption of the South Penninic ocean and subsequent collision between the AA and the Middle Penninic block occurred during post-Cretaceous

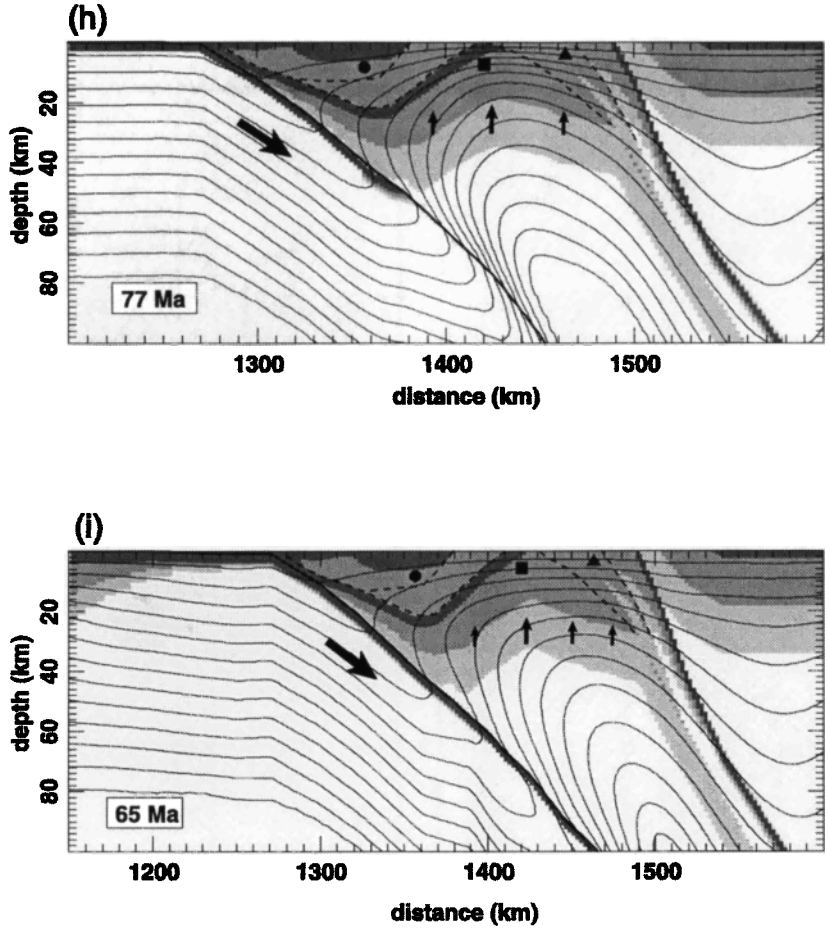

Figure 5. (continued)

times. However, subduction of the South Penninic ocean cooled the base of the orogen but did not influence the cooling history of the particular basement rocks modeled in this study.

5.4. Rheological Modeling

Modeling of the paleorheology during continent-continent collision, along the cross section described in section 4, gives important indications on the mechanical evolution of orogens [see also *van Wees et al.*, 1992; *Genser et al.*, 1996]. The mechanical structure of the lithosphere is primarily a function of its composition and temperature. Hence thermal perturbations have a significant impact on the mechanical properties of the lithosphere. Below we discuss the effect of changing thermal regimes on the rheological evolution of an orogen. Predictions on the paleorheology are made using the kinematic and heat flow assumptions discussed in section 4. Crustal compositions are chosen, taking into account the surface geology of the eastern Alps and seismic velocity studies from the Alpine part of the European Geotraverse (Table 3) [e.g., *Okaya et al.*, 1996]. Numerically modeled strength profiles are shown for selected stages, when major changes of the thermal regime occur. For a better visualization the rheological stratification of the lithosphere is displayed together with strength envelopes (e.g., Figure 4b).

Strong lateral variations in lithospheric strength are predicted for the precollisional mechanical state of the lithosphere along the cross section (Figure 4b). Strong oceanic crust in the area of the thermally relaxed South Penninic ocean passes laterally into weak continental crust of the AA domain, characterized by 6-8 km of brittle upper crust and a weak subcrustal lithosphere. Similarly strong lateral variations in lithospheric strength are predicted at the transition of the AA to the Meliata oceanic crust as well as at the position of the oceanic sediments on top of the subducting oceanic slab (Figure 4b). This particular situation suggests that the AA lower crust and its subcrustal lithosphere together form a coupled system, decoupled from the upper crust. Although weak, AA lower crust and subcrustal lithosphere are thought to be subductable, pulled down by the sinking oceanic Meliata-Hallstatt slab [see also *Chemenda et al.*, 1996]. According to our strength calculations, subduction of cold and strong oceanic lithosphere also affects the overriding continental plate, which gains strength at its leading edge (Figure 4b). In the same way, UA rocks regain strength, when they are underthrusted by the MA, the LA or the South Penninic ocean (Figures 5b, 5f, and 5g). On the other hand, exhumation-related advective upward heat transport, together with an increased heat production rate due to radioactive

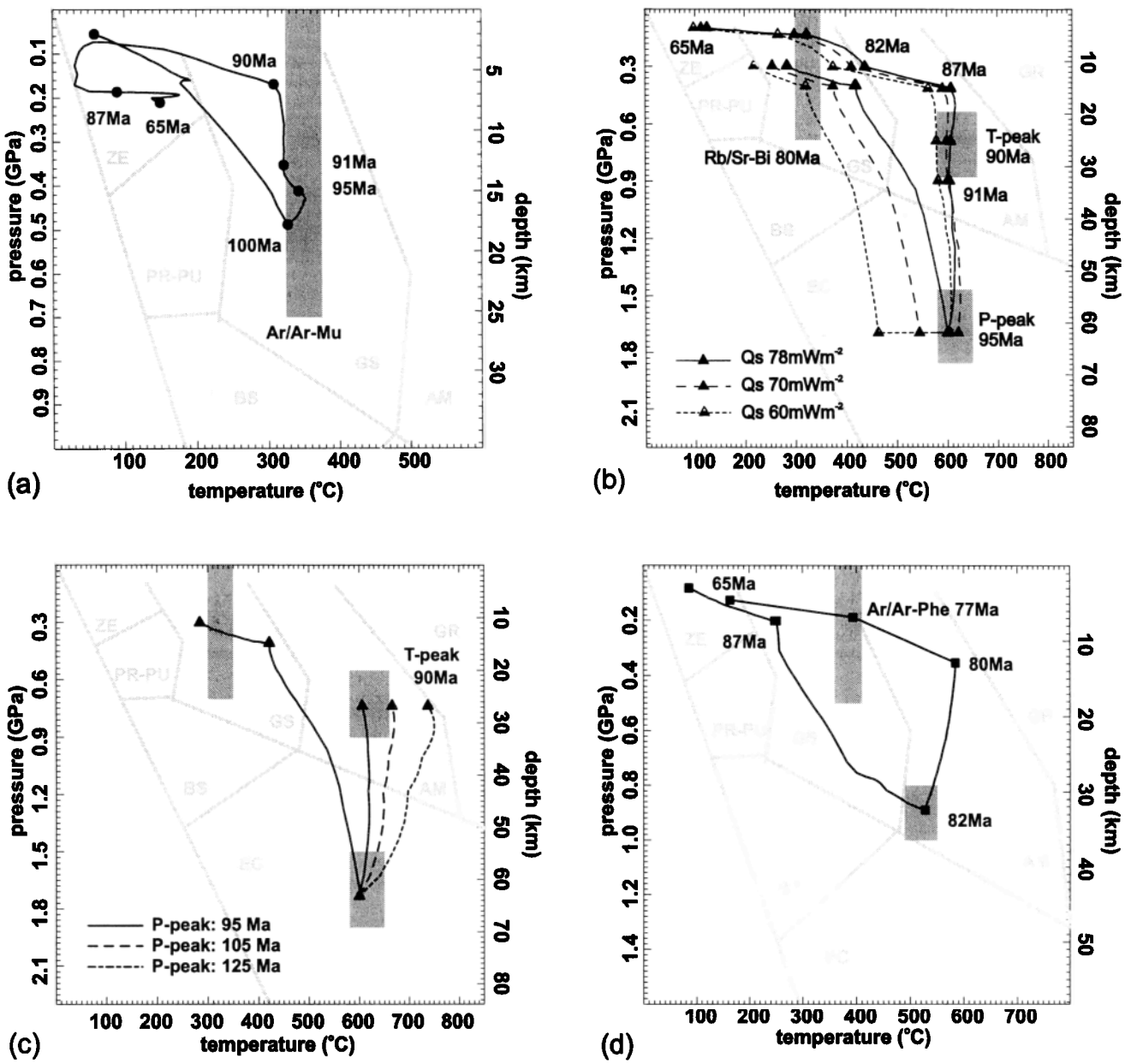

Figure 6. P-T graphs for modeled P-T paths of different tectonic units. Metamorphic facies distribution is drawn in simplified form and taken from *Spear* [1993]. Abbreviations: ZE, zeolith facies; PR-PU, prehnite-pumpellyte facies; BS, blueschist facies; GS, greenschist facies; AM, amphibolite facies; EC, eclogite facies; GR, granulite facies. All P-T graphs start at 260 Ma. Note that the first phase of burial and heating is due to deposition of Mesozoic cover series on top of the lithosphere. (a) P-T graph for the UA Graywacke Zone for the time steps as indicated. The $^{40}Ar/^{39}Ar$ closing temperature range for muscovite is taken from [1993] and based on data from *Dallmeyer et al.* [1996, 1998] and *Handler et al.* [1996]. (b) P-T paths for the MA eclogites using different heat flow assumptions. Note that an initial surface heat flow of 78 mW m^{-2} gave the best fit with the observed P-T path compiled from *Miller* [1990], *Thöni and Jagoutz* [1992], *Thöni and Miller* [1996], and *Gregurek et al.* [1997]. Age data for the metamorphic and cooling events as indicated by the boxes are compiled from *Frank et al.* [1987], *Thöni and Jagoutz* [1992], *Thöni and Miller* [1996], and *Morauf* [1982]. The closing temperature range of biotite for the Rb/Sr system is taken from *von Blanckenburg et al.* [1989]. (c) Thermal consequences in variations of timing of the high-pressure event and its influence on the exhumation path of the eclogites. Boxes are as those in Figure 6b. (d) Modeled P-T path for the southern part of the LA unit. P-T range is taken from *Moine et al.* [1989], and cooling ages are from *Dallmeyer et al.* [1996] and *Dunkl* [1992]. The closing temperature range of phengitic white micas for the $^{40}Ar/^{39}Ar$ system is taken from *von Blanckenburg et al.* [1989] and *Kohn et al.* [1995].

decay in thickened continental crust, causes weakening of the thickened orogenic system (Figures 5d and 5f). It is important to note that depending on the thermal regime, lithospheric strength can vary considerably across an orogen. Using the kinematic and thermal assumptions outlined in preceding sections, low strength is predicted in central parts of the orogen whereas the leading edge of the overriding plate represents a high-strength region.

6. Implications for Dynamics of the Austro-Alpine Unit

In this section, modeling results are discussed and compared with models based on field and laboratory data. Furthermore, an attempt is made to relate model results to orogenic processes and their possible effects on the Cretaceous evolution of the AA.

6.1. Onset of Middle Cretaceous Continent-Continent Collision

Continental collision affecting first UA units is documented by thrusting within cover as well as basement series [*Decker et al.*, 1994; *Eisbacher and Brandner*, 1995; *Dallmeyer et al.*, 1996; *Schweigl and Neubauer*, 1997]. The adopted scenario invoking southeastward underthrusting of UA units underneath the upper plate (Figure 5a) is able to account for the observed southward to southeastward increase in thermal overprint within the cover series and the very low to low grade metamorphic overprint [e.g., *Kralik et al.*, 1987; *Dallmeyer et al.*, 1996]. The use of an elevated heat flow implies the mechanically weak behavior of the continental lithosphere, allowing a complete decoupling of upper crustal rocks, which are subsequently stacked, from the rest of the lithosphere at relatively shallow crustal levels (Figures 5b and 5c). Since there are no estimates on the maximum pressures reached during greenschist facies metamorphism within the UA Graywacke Zone, it is difficult to assess how close the numerical model predictions come to "reality." However, the numerical model predicts maximum pressures of the order of 0.48 GPa, equivalent to burial depths of approximately circa 15 km. This is sufficient for the UA Graywacke Zone to induce a prograde lower greenschist facies overprint, as recorded by synkinematically grown white micas [*Dallmeyer et al.*, 1996]. According to our model calculations, subsequent exhumation of these rocks, probably triggered by the underplating of buoyant MA continental crust, is required in order not to exceed the blocking temperatures of the $^{40}Ar/^{39}Ar$ system for white mica.

6.2. Eclogite Facies Metamorphism and Exhumation of HP rocks

On the basis of radiometric age dating, *Thöni and Jagoutz* [1992] and *Thöni and Miller* [1996] argued for a "young" high-pressure event between 95 and 100 Ma (Figure 7a). They coupled their data with a P-T path that is characterized by an isothermal exhumation path terminating in an amphibolite facies metamorphic overprint around 90 Ma. Additionally, the intimate link of metamorphism and deformation was emphasized by *Stüwe* [1998]. Using the model assumptions outlined in section 4, we were able to reproduce these particular features, placing the eclogite facies metamorphism as late as 95 Ma (Figure 7a). Only fast exhumation results in an isothermal exhumation path and prevents an obliteration of the HP-mineral assemblages due to thermal re-equilibration. According to our model results, it is important to note that isothermal exhumation of the eclogites occurs within 5-10 Myr, equivalent to average exhumation rates ranging from 7.5 to 4 mm yr^{-1}, respectively. The resulting P-T path seems to be largely independent of the exhumation mechanism (thrusting versus erosion) used but strongly dependent on the velocity of the processes. This suggests that the high-pressure event was followed by the amphibolite facies overprint within a time span of 10 Myr.

In our numerical model approach we explain the P-T path related to the burial-exhumation history of the eclogites by heat conduction coupled with heat advection and radiogenic heat production. Alternatively, episodic release of heat due to syndeformational shear heating might have been an important heat source during the Cretaceous metamorphism-deformation history of the MA (for review, see *Stüwe* [1998]). Rapid exhumation of the high-pressure rocks might have been driven by the density difference of the buried continental crust and the surrounding mantle lithosphere, although transformation of the continental material to eclogites caused an increase in rock density. Analogue modeling showed that exhumation of deeply buried continental crust by buoyancy forces is able to account for very rapid movement of the rocks toward shallower crustal levels [*Chemenda et al.*, 1996].

6.3. Late Cretaceous Tectonics and Their Relationship to Gosau Basin Formation

As shown by field studies, a combination of erosion and ductile normal faulting reduced the thickness of the orogen and caused the rise of metamorphic crust [*Ratschbacher et al.*, 1989; *Neubauer et al.*, 1992b; 1995]. Coevally, extensional basins (Gosau basins) formed on top of the thickened lithosphere [e.g., *Neubauer et al.*, 1995].

Our modeling gives important implications for possible mechanisms underlying the formation of Gosau basins during the Late Cretaceous. As shown by the numerical model predictions, synorogenic extensional tectonics together with erosion have the potential to increase the geotherm significantly (Figure 5g). Therefore a very rapid increase of temperature with depth, coupled with a shift of the brittle-ductile transition to relatively shallow crustal levels can mimic a large break of metamorphic grade between rock units. In the case of the AA nappe edifice the numerical model predictions suggest that the observed metamorphic break and the break in deformation behavior between the MA unit of the Koralpe and Gleinalpe region and the overlying UA Graz Paleozoic unit do not require the excision of large quantities of crustal material.

Pronounced lateral gradients in temperature and strength of the rocks can be observed along the modeled cross section. In areas of high synorogenic heat flow a decrease in rock density is expected to occur, probably facilitating buoyancy-driven exhumation of the rocks. However, it is important to note that the model predicts very weak lithosphere where the continental crust is most piled up [see also *Genser et al.*,

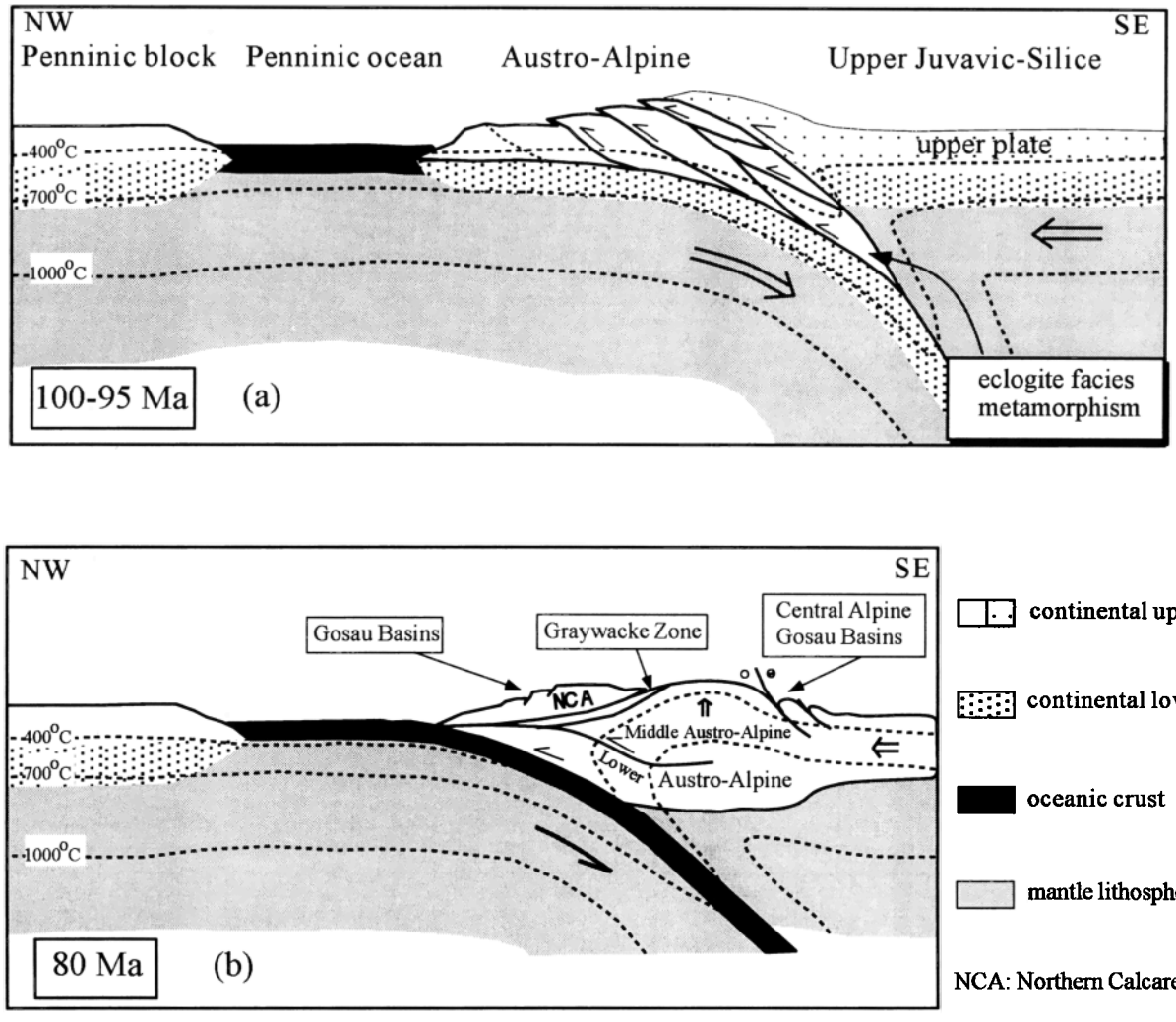

Figure 7. Cartoon showing key stages in the evolution of the AA realm inferred from modeling and geological constraints: (a) Middle to early Late Cretaceous nappe stacking and (b) Late Cretaceous extension.

1996; *Okaya et al.*, 1996]. We therefore suggest that the AA continental crust was probably not able to support large stresses and collapsed (Figure 7b). This is expressed by the Late Cretaceous E-W directed extension although the system as a whole was still converging [*Ratschbacher et al.*, 1989].

In this context the opening of the extensional Gosau basins is of particular interest, because no unique basin-forming mechanism seems to be able to account for the basic geological features observed [e.g., *Wagreich and Faupl*, 1994; *Wagreich*, 1995]. Opening of Gosau basins on top of the Northern Calcareous Alps is dominated by strike-slip deformation [*Wagreich*, 1993; 1995]. An important regressional and erosional phase, separating the Lower Gosau group from the Upper Gosau group was mapped by *Faupl et al.* [1987] and *Wagreich* [1993; 1995]. In our numerical model approach we relate this uplift to progressive underthrusting of buoyant LA continental crust. We attribute subsequent tilting of the Northern Calcareous Alps and renewed subsidence of Gosau basins circa 84-70 Myr to the removal of the LA crust from its northern margin position [*Neubauer*, 1994b] and not to subcrustal tectonic erosion as postulated by *Wagreich* [1993]. In contrast, more internal parts of the orogen are thickened again by accretion of the LA unit. We therefore relate the major subsidence pulse in central Alpine Gosau basins (see also Figure 1) during the lower Campanian (approximately 82-80 Myr ago) to the collapse of the AA crust.

If we compare the modeled crustal thickness before the collisional event with that predicted at the end of the Cretaceous, we have to realize that they are close to equal (compare Figures 4a and 5i), suggesting that ductile thinning of the AA crust and erosion left behind an only slightly thickened continental crust by the end of the Cretaceous.

The role of the South Penninic ocean during the Cretaceous was twofold: (1) Cooling of the hanging-wall by underplating could have been accompanied by cooling related to the dehydration of water-saturated oceanic sediments and their subsequent infiltration into the hangingwall basement. This process, expressed by the formation of white schists [e.g., *Moine et al.*, 1989], would probably facilitate the release of

heat compared to heat conduction only. (2) The mechanically strong and already cold oceanic crust (Figures 4a and 5f) is suitable to transmit stresses, leading to far-field compressional deformation in the European foreland (Bohemian Massif) due to collisional coupling of the Alpine orogen with the European foreland from circa 80 Myr onward [*Ziegler et al.*, 1995, 1998].

7. Conclusions

On the basis of our numerical model results and geological constraints, we conclude that (1) the P-T-t history of the AA part of the eastern Alps can be explained by Cretaceous continent-continent collision and related imbrication of AA tectonic units, (2) HP metamorphism probably occurred as late as 95 Ma, (3) exhumation rates between 4 and 7.5 mm y^{-1} are consistent with isothermal exhumation of the eclogites within MA units, most likely related to a combination of tectonic and erosional unroofing, (4) amphibolite facies metamorphic conditions within southern MA units are reached at the end of the isothermal exhumation phase, (5) underplating of the LA unit was followed by rapid postmetamorphic exhumation, (6) major subsidence in central Alpine Gosau basins was probably due to the collapse of very weak and thickened continental crust, (7) rocks of the AA nappe complex, exposed at present, already reached a near-surface position at the end of the Cretaceous, and (8) lateral variations in lithospheric strength play an important role both during the buildup and dismembering of the AA nappe complex and in the context of collision-related foreland deformation.

Acknowledgments. K. Stüwe and S. Ellis are thanked for their careful reviews and suggestions to improve the manuscript. R.A. Stephenson and P.A. Ziegler are thanked for useful discussions. Funding of this work by the European Commission, TMR-project ERBFMBICT950297 is gratefully acknowledged by the first author. This is publication 990108 of the Netherlands Research School of Sedimentary Geology (NSG).

References

Behrmann, J., and L. Ratschbacher, Archimedes revisited: A structural test of eclogite emplacement models in the Austrian Alps, *Terra Nova, 1*, 242-252, 1989.

Behrmann, J.H., Zur Kinematik der Kontinentkollision in den Ostalpen, *Geotekton. Forsch., 76*, 1-180, 1990.

Buck, W.R., F. Martínez, M.S. Steckler, and J.R. Cochran, Thermal consequences of lithospheric extension: Pure and simple, *Tectonics, 7*, 213-234, 1988.

Carter, N., and M. Tsenn, Flow properties of continental lithosphere, *Tectonophysics, 136*, 27-63, 1987.

Channell, J.E.T., and H.W. Kozur, How many oceans? Meliata, Vardar and Pindos oceans in Mesozoic Alpine paleogeography, *Geology, 25*, 183-186, 1997.

Chemenda, A.I., M. Mattauer, and A.N. Bokun, Continental subduction and a mechanism for exhumation of high-pressure metamorphic rocks: New modelling and field data from Oman, *Earth Planet. Sci. Lett., 143*, 173-182, 1996.

Dallmeyer, R.D., F. Neubauer, R. Handler, H. Fritz, W. Müller, W. Antonitsch, and S. Herman, $^{40}Ar/^{39}Ar$ and Rb-Sr mineral age control for the pre-Alpine and Alpine tectonic evolution of the Austro-Alpine Nappe complex, eastern Alps, *in ALCAPA: Field Guide*, pp. 47-59, IGP/KFU Graz, Austria, 1992.

Dallmeyer, R.D., F. Neubauer, R. Handler, H. Fritz, W. Müller, D. Pana, and M. Putis, Tectonothermal evolution of the internal Alps and Carpathians: Evidence from $^{40}Ar/^{39}Ar$ mineral and whole-rock data, *Eclogae Geol. Helv., 89*, 203-227, 1996.

Dallmeyer, R.D., R. Handler, F. Neubauer, and H. Fritz, Sequence of thrusting within a thick-skinned tectonic wedge: Evidence from $^{40}Ar/^{39}Ar$ and Rb-Sr ages from the Austroalpine nappe complex of the eastern Alps, *J. Geol., 106*, 71-86, 1998.

Davy, P., and P. Gillet, The stacking of thrust slices in collisional zones and its thermal consequences, *Tectonics, 5*, 913-929, 1986.

Decker, K., H. Peresson, and P. Faupl, Die miozäne Tektonik der östlichen Kalkalpen: Kinematik, Paläospannungen und der Deformationsablaufteilung während der "lateralen Extrusion" der Zentralalpen., *Jahrb. Geol. Bundesanst. Austria, 137*, 5-18, 1994.

Dingeldey, C., R.D. Dallmeyer, F. Koller, and H.-J. Massonne, P-T-t history of the Lower Austroalpine Nappe Complex in the "Tarntaler Berge" NW of the Tauern Window: Implications for the geotectonic evolution of the central eastern Alps, *Contrib. Mineral. Petrol., 129*, 1-19, 1997.

Dunkl, I., Final episodes of the cooling history of eastern termination of the Alps, *in ALCAPA: Field Guide*, pp. 137-139, IGP/KFU Graz, Austria, 1992.

Ehlers, K., K. Stüwe, R. Powell, M. Sandiford, and W. Frank, Thermometrically inferred cooling rates from the Plattengneis, Koralm region, Eastern Alps, *Earth Planet. Sci. Lett., 125*, 307-321, 1994.

Eisbacher, G.H., and R. Brandner, Role of high-angle faults during heteroaxial contraction, Inntal thrust sheet, Northern Calcareous Alps, Western Austria, *Geol. Paläontol. Mitt., 20*, 389-406, 1995.

Faupl, P., E. Pober, and M. Wagreich, Facies development of the Gosau Group of the eastern parts of the Northern Calcareous Alps during the Cretaceous and Paleogene, in *Geodynamics of the Eastern Alps*, edited by H.W. Flügel and P. Faupl, pp. 142-155, Deuticke, Vienna, 1987.

Frank, W., Evolution of the Austroalpine elements in the Cretaceous, in *Geodynamics of the Eastern Alps*, edited by H.W. Flügel and P. Faupl, pp. 379-406, Deuticke, Vienna, 1987.

Frank, W., M. Esterlus, I. Frey, G. Jung, A. Krohe, and J. Weber, Die Entwicklungsgeschichte von Stub- und Koralpen Kristallin und die Beziehung zum Grazer Paläozoikum, *Jahresber. Hochschulschwerpunkt S15, 4*, 263-293, 1983.

Frank, W., P. Klein, W. Nowy, and S. Scharbert, Die Datierung geologischer Ereignisse im Altkristallin der Gleinalpe (Steiermark) mit der Rb/Sr-Methode, *Tschermaks Mineral. Petrogr. Mitt., 23*, 191-203, 1976.

Frank, W., M. Kralik, S. Scharbert, and M. Thöni, Geochronological data from the eastern Alps, in *Geodynamics of the Eastern Alps*, edited by H.W. Flügel and P. Faupl, pp. 272-281, Deuticke, Vienna, 1987.

Frey, M., J. Desmons, and F. Neubauer, Metamorphic map of the Alps, *Schweiz. Mineral. Petrogr. Mitt., 79*, 1-4, 1999.

Frisch, W., Tectonic progratation and plate tectonic evolution of the Alps, *Tectonophysics, 60*, 121-139, 1979.

Fritz, H., Kinematics and geochronology of Early Cretaceous thrusting in the northwestern Paleozoic of Graz (Eastern Alps), *Geodin. Acta, 2*, 53-62, 1988.

Froitzheim, N., S.M. Schmid, and M. Frey, Mesozoic paleogeography and the timing of eclogite-facies metamorphism in the Alps: A working hypothesis, *Eclogae. Geol. Helv., 89*, 81-110, 1996.

Gawlik, H.J., Die früh-oberjurassischen Brekzien der Strubbergschichten im Lammertal-Analyse und tektonische Bedeutung (Nördlichen Kalkalpen, Österreich., *Mitt. Ges. Geol. Bergbaustud. Österr., 39/40*, 119-186, 1996.

Genser, J., Rheological controls on the evolution of a collisional orogene, *Terra Nova Abstr., 5*, 258, 1993.

Genser, J., J.D. van Wees, S. Cloetingh, and F. Neubauer, Eastern Alpine tectono-metamorphic evolution: constraints from two-dimensional P-T-t modeling, *Tectonics, 15*, 584-604, 1996.

Gregurek, D., R. Abart, and G. Hoinkes, Contrasting Eoalpine P-T evolutions in the southern Koralpe, eastern Alps, *Mineral. Petrol., 60*, 61-80, 1997.

Handler, R., R.D. Dallmeyer, F. Neubauer, and H. Fritz, Sequence of thrusting within a thick-skinned tectonic: The example of the Austroalpine nappe complex, eastern Alps, paper presented at the 6. Tektonik-Strukturgeologie-Kristallingeologie (TSK) Symposium, *Erweiterte Kurzfassungen*, Salzburg, Austria, 162-165, 1996.

Hawkesworth, C.J., D.J. Waters, and M.J. Bickle, Plate tectonics in the eastern Alps, *Earth Planet. Sci. Lett., 24*, 405-413, 1975.

Hejl, E., "Cold spots" during the Cenozoic evolution of the eastern Alps: Thermochronological interpretation of apatite fission-track data, *Tectonophysics, 272*, 159-174, 1997.

Hoinkes, G., A. Kostner, and M Thöni, Petrologic constraintes for Eoalpine eclogite facies metamorphism in the Austroalpine Ötztal Basement, *Mineral. Petrol., 43*, 237-254, 1991.

Hoke, L., The Altkristallin of the Kreuzeck Mountains, SE Tauern Window, eastern Alps: Basement crust in a convergent plate boundary zone, *Jahrb. Geol. Bundesanst. Austria, 133*, 5-87, 1990.

Inger, S., and R.A. Cliff, Timing of metamorphism in the Tauern Window, eastern Alps: Rb-Sr ages and fabric formation, *J. Metamorph. Geol., 12*, 695-707, 1994.

Kohn, M.J., F.S. Spear, T.M. Harrison, and I.W.D. Dalziel, $^{40}Ar/^{39}Ar$ geochronology and P-T-t paths from the Cordillera Darwin metamorphic complex, Tierra del Fugo, Chile, *J. Metamorph. Geol., 13*, 251-270, 1995.

Kozur, H., The evolution of the Meliata-Hallstatt Ocean and its significance for the early evolution of the eastern Alps and western Carpathians, *Palaeogeogr. Palaeoclimatol. Palaeoecol., 87*, 109-135, 1991.

Kralik, M., H. Krumm, and M. Schramm, Low grade and very low grade metamorphism in the Northern Calcareous Alps and in the Greywacke zone: Illite-crystallinity data and isotopic ages, in *Geodynamics of the Eastern Alps*, edited by H.W. Flügel and P. Faupl, pp. 164-178, Deuticke, Vienna, 1987.

Krohe, A., Kinematics of Cretaceous nappe tectonics in the Austroalpine basement of the Koralpe region (eastern Austria), *Tectonophysics, 136*, 171-196, 1987.

Kurz, W., F. Neubauer, and J. Genser, Kinematics of Penninic nappes (Glockner Nappe and basement-cover nappes) in the Tauern Window (eastern Alps, Austria) during subduction and Penninic-Austroalpine collision, *Eclogae Geol. Helv., 89*, 573-605, 1996.

Kurz, W., F. Neubauer, J. Genser, and E. Dachs, Alpine geodynamic evolution of passive and active continental margin sequences in the Tauern Window (eastern Alps, Austria, Italy): A review, *Geol. Rundsch., 87*, 225-242, 1998.

Lein, R., Evolution of the Northern Calcareous Alps during Triassic times, in *Geodynamics of the Eastern Alps*, edited by H.W. Flügel and P. Faupl, pp. 85-102, Deutike, Vienna, 1987.

Miller, C., Petrology of the typt-locality eclogites from the Koralpe and Saualpe (eastern Alps), Austria, *Schweiz. Mineral. Petrogr. Mitt., 70*, 287-300, 1990.

Moine, B., J.P. Fortune, P. Moreau, and F. Viguer, Comparative mineralogy, geochemistry and conditions of formation of two metasomatic talc and chlorite deposits: Trimouns (Pyrenees France) and Rabenwald (eastern Alps, Austria), *Econ. Geol., 84*, 1398-1416, 1989.

Morauf, W., Rb-Sr und K-Ar-Evidenz für eine intensive alpidische Beeinflussung der Paragesteine in Kor- und Saualpe, SE-Ostalpen, Österreich., *Tschermaks Mineral. Petrogr. Mitt., 29*, 255-282, 1982.

Neubauer, F., Kontinentkollision in den Ostalpen, *Geowissenschaften, 12*, 136-140, 1994a.

Neubauer, F., Subcrustal tectonic erosion in orogenic belts: A model for the Late Cretaceous subsidence of the Northern Calcareous Alps (Austria): Comment, *Geology, 22*, 855-856, 1994b.

Neubauer, F., W. Müller, P. Peindl, G. Moyschewitz, E. Wallbrecher, and M. Thöni, Evolution of lower Austroalpine units along eastern margins of the Alps, *in ALCAPA: Field Guide*, pp. 97-114, IGP/KFU Graz, Austria, 1992a.

Neubauer, F., J. Genser, H. Fritz, and E. Wallbrecher, Alpine kinematics of the eastern Central Alps, *in ALCAPA: Field Guide*, pp. 127-136, IGP/KFU Graz, Austria, 1992b.

Neubauer, F., R.D. Dallmeyer, I. Dunkl, and D. Schirnik, Late Cretaceous exhumation of the metamorphic Gleinalm dome, eastern Alps: Kinematics, cooling history and sedimentary response in a sinistral wrench corridor, *Tectonophysics, 242*, 79-89, 1995.

Neubauer, F., R.D. Dallmeyer, and A. Takasu, Conditions of eclogite formation and age of retrogression within the Sieggraben unit, eastern Alps: Implications for Alpine-Carpathian tectonics, *Schweiz. Mineral. Petrogr. Mitt., 79/2*, 297-307, 1999.

Oberhauser, R., Zur Kenntnis der Tektonik und der Paläogeographie des Ostalpenraumes zur Kreide-, Paleozän- und Eozänzeit, *Jahrb. Geol. Bundesanst. Austria., 138*, 369-432, 1995.

Okaya, N., S. Cloetingh, and S. Müller, A lithospheric cross section through the Swiss Alps, Constraints on the mechanical structure of a continent-continent collision zone, *Geophys. J. Int., 127*, 399-414, 1996.

Pollack, H.N., and D.S. Chapman, On the regional variation of heat flow, geotherms and lithospheric thickness, *Tectonophysics, 38*, 279-296, 1977.

Ratschbacher, L., W. Frisch, F. Neubauer, S.M. Schmid, and J. Neugebauer, Extension in compressional orogenic belts: The eastern Alps, *Geology, 17*, 404-407, 1989.

Reddy, S.M., R.A. Cliff, and R. East, Thermal history of the Sonnblick Dome, South-east Tauern Window, Austria: Implications for heterogeneous uplift within the Pennine basement, *Geol. Rundsch., 82*, 667-675, 1993.

Schweigl, J., and F. Neubauer, Structural evolution of the central Northern Calcareous Alps: Significance for the Jurassic to Tertiary geodynamics in the Alps, *Eclogae Geol. Helv., 90*, 303-323, 1997.

Spear, F.S., *Metamorphic Phase Equilibria and Pressure-Temperature-Time Paths*, 799 pp., Mineral. Soc. Am., Washington, D.C., 1993.

Stüwe, K., Heat sources of Cretaceous metamorphism in the aastern Alps: A discussion, *Tectonophysics, 287*, 251-269, 1998.

Stüwe, K., and R. Powell, P-T paths from modal proportions: Applications to the Koralm Complex, eastern Alps, *Contrib. Mineral. Petrol., 119*, 83-93, 1995.

Stüwe, K., and M. Sandiford, Mantle-lithospheric deformation and crustal metamorphism with some speculations on the thermal and mechanical significance of the Tauern event, eastern Alps., *Tectonophysics, 242*, 115-132, 1995.

Thöni, M., Rb-Sr isotopic resetting in mylonites and pseudotachylites: Implications for the detachment and thrusting of the Austroalpine basement nappes in the eastern Alps, *Jahrb. Geol. Bundesanst. Austria, 131*, 169-201, 1988.

Thöni, M., and G. Hoinkes, Geochronological and petrological consequences of Eoalpine metamorphic overprinting, in *Geodynamics of the Eastern Alps*, edited by H.W. Flügel and P. Faupl, pp. 200-213, Deutike, Vienna, 1987.

Thöni, M., and E. Jagoutz, Some new aspects of dating eclogites in orogenic belts: Sm-Nd, Rb-Sr and Pb-Pb isotopic results from the Austroalpine Saualpe and Koralpe type-locality (Carinthia/Styria, southeastern Austria), *Geochim. Cosmochim. Acta, 56*, 347-368, 1992.

Thoni, M., and E. Jagoutz, Isotopic constraints for eo-Alpine high-P metamorphism in the Austroalpine nappes of the eastern Alps' Bearing on Alpine orogenesis, *Schweiz. Mineral. Petrogr. Mitt., 73*, 177-189, 1993.

Thoni, M., and C. Miller, Garnet Sm-Nd data from the Saualpe and the Koralpe (eastern Alps, Austria): Chronological and P-T constraints on the thermal and tectonic history, *J. Metamorph. Geol., 14*, 453-466, 1996.

Tollmann, A., *Geologie von Österreich*, 766 pp., Deuticke, Vienna, 1977.

Tollmann, A., Grosstecktonische Ergebnisse aus den Ostalpen im Sinne der Plattentektonik, *Mitt. Oesterr. Geol. Ges., 71/72*, 37-44, 1980.

Tollmann, A., The alpidic evolution of the eatern Alps, in *Geodynamics of the Eastern Alps*, edited by H.W. Flügel and P. Faupl, pp. 361-378, Deuticke, Vienna, 1987.

van Wees, J.D., K. de Jong, and S. Cloetingh, Two-dimensional P-T-t modelling and the dynamics of extension and inversion in the Betic Zone (SE Spain), *Tectonophysics, 203*, 305-324, 1992.

Voll, G., Seriengliederung, Gefügeentwicklung und Metamorphosein den Nördlichen Radstätter Tauern zwischen Forstau- und Preunegg-Tal, paper presented at the Geodynamics and Geotraverses Around the Alps Conference, *Abstr. vol.*, Salzburg, Austria, pp. 1-2, 1977.

von Blanckenburg, F., and J.H. Davies, Feasibility of double slab breakoff (Cretaceous and Tertiary) during the Alpine convergence, *Eclogae Geol. Helv., 89*, 111-127, 1996.

von Blanckenburg, F., I.M. Villa, H. Baur, G. Morteani, and R.H. Steiger, Time calibration of a P-T-path from the Western Tauern Window, eastern Alps: The problem of closure temperatures, *Contrib. Mineral. Petrol., 101*, 1-11, 1989.

von Eynatten, H., R. Gaupp, and J.R. Wijbrans, $^{40}Ar/^{39}Ar$ laser-probe dating of detrital white micas from Cretaceous sedimentary rocks of the eastern Alps: Evidence for Variscan high-pressure metamorphism and implications for Alpine orogeny, *Geology, 24*, 691-694, 1996.

Wagreich, M., Subcrustal tectonic erosion in orogenic belts: A model for the Late Cretaceous subsidence of the northern Calcareous Alps (Austria), *Geology, 21*, 941-944, 1993.

Wagreich, M., Subduction tectonic erosion and Late Cretaceous subsidence along the northern Austroalpine margin (eastern Alps, Austria), *Tectonophysics, 242*, 63-78, 1995.

Wagreich, M., and P. Faupl, Paleogeography and geodynamic evolution of the Gosau Group of the Northern Calcareous Alps (Late Cretaceous, eastern Alps, Austria), *Palaeogeogr., Palaeoclimatol., Palaeoecol., 110*, 235-254, 1994.

Weber, J., Metamorphosestudien an pelitischen Gesteinen der Wolfsberger Serie und der tieferen Anteile des Koralpenkristallins in Kärnten, unpubl. Ph.D thesis, Institut für Geologie, University of Vienna, Austria, 1982.

Wieseneder, H., Gesteinsserien und Metamorphose im Ostabschnitt der österreichischen Zentralalpen, *Verh. Geol. Bundesanst. Austria, 2*, 344-357, 1972.

Wijbrans, J.R., J.D. van Wees, R.A. Stephenson, and S.A.P.L. Cloetingh, Pressure-temperature-time evolution of the high-pressure metamorphic complex of Sifnos, Greece, *Geology, 21*, 443-446, 1993.

Ziegler, P.A., S. Cloetingh, and J.D. van Wees, Dynamics of intra-plate compressional deformation: The Alpine foreland and other examples, *Tectonophysics, 252*, 7-59, 1995.

Ziegler, P.A., J.D. van Wees, and S. Cloetingh, Mechanical controls on collision-related compressional intraplate deformation, *Tectonophysics, 300*, 103-129, 1998.

S.A.P.L. Cloetingh, J.D. van Wees, and E. Willingshofer, Faculty of Earth Sciences, Vrije Universiteit, De Boelelaan 1085, 1081 HV Amsterdam, Netherlands. (wile@geo.vu.nl)

F. Neubauer, Institut für Geologie und Paläontologie, Universität Salzburg, Hellbrunnerstrasse 34, 5020 Salzburg, Austria.

(Received March 2, 1998;
revised March 4, 1999;
accepted March 30, 1999.)